BB

ISSN 1346-244X
RIKEN-AF-NP-395

Neutron pair pre-emission in the fusion of ^{11}Li halo nuclei with Si targets

M. Petrascu, I. Tanihata, T. Kobayashi, M. Giurgiu, K. Morimoto, K. Katori, I. Cruceru, A. Isbasescu, H. Petrascu, R. Ruscu, M. Chiba, Y. Nishi, S. Nishimura, A. Ozawa, T. Suda, K. Yoshida, A. Constantinescu, C. Bordeanu, and A. Tudorica

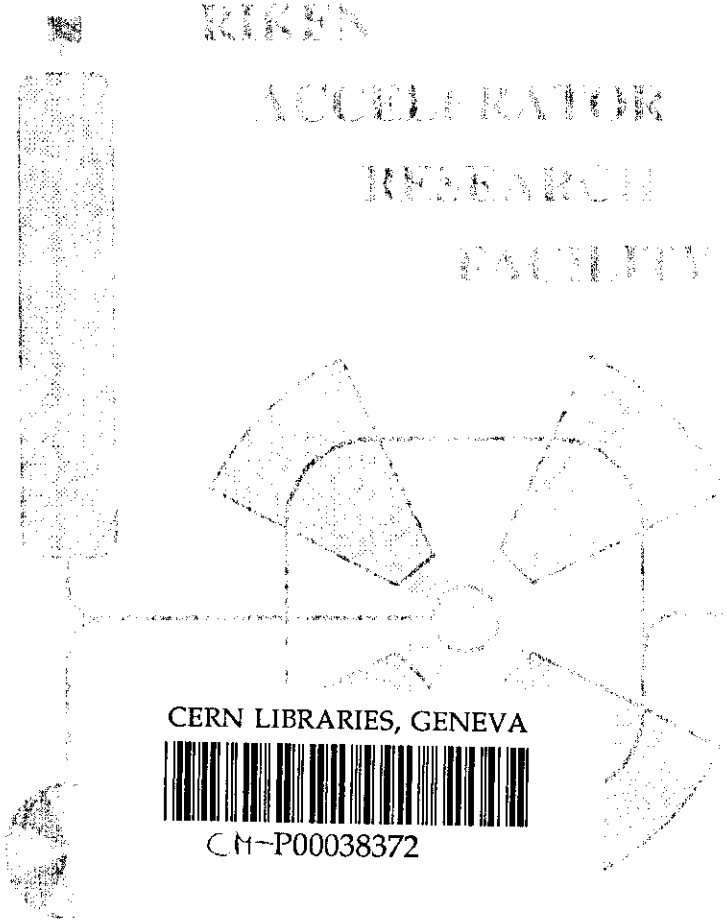

April 2001

The Institute of Physical and Chemical Research (RIKEN)
2-1 Hirosawa, Wako, Saitama 351-0198, Japan
TEL: (048)462-1111 FAX: (048)462-4642
e-mail: *username*@rikvax.riken.go.jp

Preliminary (internal use)

Neutron pair pre-emission in the fusion of ^{11}Li halo nuclei with Si targets

M.Petrascu[1], I.Tanihata[2], T. Kobayashi[3], M.Giurgiu[2], K.Morimoto[2], K.Katori[2], I.Cruceru[1], A. Isbasescu[1], H.Petrascu[1], R.Ruscu[1], M.Chiba[2], Y. Nishi[2], S. Nishimura[2], A.Ozawa[2], T. Suda[2], K.Yoshida[2], A. Constantinescu[4], C.Bordeanu[5], A.Tudorica[6]

[1)] *Institute of Physics and Nuclear Engineering, POB MG-6, Bucharest, Romania*
[2)] *The Institute of Physical and Chemical Research (RIKEN), Hirosawa 2-1, Wako-shi, Saitama, Japan*
[3)] *Tohoku University, Japan*
[4)] *Bucharest University, Romania*
[5)] *Weizmann Institute, Rehovot, Israel*
[6)] *SUNY at Stony Brook, Chemistry Dept, NY-11774, USA*

Abstract

The pre-emission of neutron pairs in the fusion of ^{11}Li halo nuclei with Si targets, was first mentioned in ref. [3,5]. However the statistics of n-n coincidences was rather low due to the fact that the detection system was not optimal for such measurements. Here, we report results of a recent experiment performed by the aid of a new array detector, revealing a notable n-n coincidence effect. After subtraction of the cross-talk background, a number of about 300 n-n coincidences remained within the range of the narrow neutron group. The measurement with the array detector allowed a new determination with increased resolution of the transverse momentum distribution for the neutrons within the narrow group. The best fit of the experimental data was obtained by including a background term in the Gauss function. In this case the transverse momentum $p_\perp$ expressed by σ of the distribution is $p_\perp \approx 6 \pm 1.2$ MeV/c. About 2 times larger value of σ was obtained by forcing the fit without a background term. The n-n coincidence data processed by considering a background on which the narrow neutron group is superposed allowed to obtain for P_{nn}, the percentage for neutron pair pre-emission, the value P_{nn}=(72 $\pm$ 10)%. Without subtraction of this background P_{nn} turns out to be P_{nn}=(22 $\pm$ 3)%. From the coincidence results, also the differential $d^2\sigma_{nn}(\theta_1,\theta_2)/d\Omega_1 d\Omega_2$ cross-section, for 2 neutron pre-emission was obtained. It was found that the $d^2\sigma_{nn}(\theta_1,\theta_2)/d\Omega_1 d\Omega_2$ values are close to the slope characterizing the neutron transverse momentum distribution. In contrast to the n-n coincidence data, the cross-talk data processed in the same manner for getting the cross-sections, are totally in disagreement with the slope of the neutron transverse momentum distribution. It was also observed a change in the slope of n-n coincidence data, by interchanging det #1 with det #2,4,6,8 and #3,5,7,9. This may be an indication for n-n correlation.

PACS codes: 25.60.-t, 25.60.Pj, .27.20. +n, 29.40.Mc

Keywords: NUCLEAR REACTION Si(^{11}Li, fusion); measured neutron pair pre-emission in forward direction, deduced transverse momentum distribution.

1. Introduction

The neutron halo nuclei were discovered by I. Tanihata and coworkers [1]. These nuclei are characterized by very large matter radii, small separation energies, and small internal momenta of valence neutrons.

Recently it was predicted [2] that, due to the very large dimension of ^{11}Li, one may expect that in a fusion process on a light target, the valence neutrons may not be absorbed together with the ^{9}Li core, but may be emitted in the early stage of the reaction. Indeed, the experimental investigations of neutron pre-emission in the fusion of ^{11}Li halo nuclei with Si targets [3-9], have shown that a fair amount of fusions (40 ± 12)% are preceded by one or two halo neutron pre-emission.

It was also found that in the position distribution of the pre-emitted neutrons, a very narrow neutron group, leading to transverse momentum distribution much narrower than that predicted by COSMA [12] model, is present. Some evidence based on preliminary n-n coincidence measurements, concerning the presence of neutron pairs within the narrow neutron group, has been mentioned in ref. [8,11]. In the light of this evidence, the narrow neutron distribution could be caused by the quantum interference [13,14] between two neutrons coherently pre-emitted in the fusion process. The question why such an effect is not seen in a usual breakup of ^{11}Li is answered by the fact that in this case, the coherence is destroyed by the resonant states in ^{10}Li. In the fusion process these resonant states are avoided due to the very fast disappearance of the projectile core. This view is supported by a more elaborated coincidence analysis of ref. [8]. The results of this analysis are shown in Fig. 10 of ref. [8]. Although the statistics of coincidences in Fig. 10 is poor, nevertheless it is a support for neutron pair pre-emission within the narrow neutron group. Therefore on the basis of these first results, it was decided to perform a new experiment aiming to investigate the neutron pair pre-emission in conditions of much higher statistics, by means of a neutron array [10] detector.

2. Method of the experiment

The experimental arrangement is shown in Fig.1. In this arrangement, three main parts are present:

1. The first part contains the detectors used for the control, identification and determination of the beam characteristics: a thin scintillator mounted at the F2 focus of the RIPS, two parallel plate avalanche counters (PPAC1, PPAC2), two removable detectors (3mm-Si, 0.5 mm scintillator), and a Veto1 scintillator, provided with a 2x2 cm^2 hole.

2. The second part consists of a Multiple Sampling Ionization Chamber (MUSIC), containing inside a 500 μm thick strip silicon detector-target (SiS) and a Veto2 Si detector, 200 μm thick. The anode of MUSIC is made of 10 pads. The chamber was filled with P10 gas at a pressure of 300 torr. The window was made of thin polypropylene foil. The MUSIC was used for the identification of the inclusive evaporation residues spectra produced in the detector-target, and for suppression of the energy degraded beam particle background.

3. The third part is the neutron array detector [10]. It consists of 81 detectors, made of 4 x 4 x12 cm^3 BC-400 crystals, mounted on XP2972 phototubes . This detector placed in forward direction at 138 cm from the target, was used for the energy and position determination of the neutrons originating from the target. A view of this detector is shown in Picture 1.

As a trigger in this experiment, the coincidences $F2 * PPAC2 * \overline{Veto1} * SiS * \overline{Veto2}$ were chosen. With this condition, by applying the proper gates in processing of the data, one could investigate inclusively the ^{9,11}Li +Si fusion, by considering the events produced by the incoming beam inside the detector-target. The large 5x5 cm^2 silicon Veto2 detector placed behind the Si-strip target detector, eliminated the elastic, inelastic, and breakup processes at forward angles. The contribution of elastic and inelastic processes at backward angles is expected to be very low. Calculations by the aid of programs GENOA and ECIS are confirming this expectation. The measurements were performed with ^{11}Li and ^{9}Li beams with energy centered at 13A MeV (at the entrance into target).

3. Experimental results

3.1 The inclusive spectra of fusion products

In processing of the experimental data, a gate on time of flight between scintillator F2 and PPAC2 was applied to select the energy of the incident beams. In Fig. 2, the fusion inclusive spectra for ^{11}Li beam in the 12.2–14.2 AMeV energy range and gated by 6-16 MeV neutron energy range (Fig 2-a), and by 0.7-6 MeV neutron energy range (Fig 2-b) are shown. The distributions in Fig. 2-a and 2-b, analyzed by gaussians, correspond to very close x_c (center of the gaussian) values (55.48 MeV and 56.14 MeV) This means that in both neutron energy ranges, the basic interaction process is the same. The values of x_c, could be reproduced within about 2-3 MeV by Monte Carlo fusion calculation [15], taking into account the mean energy dissipated into the target by the incoming beam particle and the mean energy dissipated by the evaporated alpha particles and protons. The obtained x_c values in the present experiment are higher than the values measured in the previous experiment, due to the fact that in the present experiment a 2 time thicker detector-target was used.

3.2 The n-n coincidences

In Fig. 3, the distribution of neutrons resulted from Si(^{11}Li , fusion), detected by 80 array elements is shown. The beam energy range between 12.2 – 14.2A MeV (at the target entrance) was selected by time of flight from F2 to PPAC2 (see Fig.1). The neutron energy was selected between 6 and 16 MeV, by time of flight on 138 cm path between the target and the array detector. As one can see in Fig. 3, there is a very pronounced peak in forward direction. The highest peak corresponds to the central #1 detector (215 counts). This number is about three times higher than the mean number of detected neutrons corresponding to the outer contour of the array (64 counts).

The distribution of neutrons from ^{9}Li-fusion is shown in Fig. 4. The statistics of counts is about 2 times lower in Fig. 4 than in Fig. 3. The distribution in Fig.4 is almost uniform, without any pronounced tendency in the forward direction. It was shown in ref. [3,5], that the neutrons from Si(^{9}Li, fusion) are predominantly of evaporation origin and since the evaporated neutrons are distributed in 4π, there is a very low probability (less than 10^{-3}) that 2 neutrons fall at the same time on the array detector. Therefore the measurement with ^{9}Li beam was used for cross-talk background determination. In Fig. 5 it is explained how the cross-talk coefficients were obtained for different coincidence orders (first, second, 3-rd, etc). The obtained cross-talk coefficients are mentioned in tables 1- 4.

The results on n-n coincidences with ^{11}Li beam are summarized in tables 1-3. These data are based on the central #1 - #9 detectors, which were used for coincidence conditioning. One can see in Tables 1-3, that there is a well defined n-n coincidence effect, much above the standard errors for all coincidence types considered (first, second and 3-rd orders). The total net number of measured coincidences is 314±30. This number corresponds to the investigated area: of 7 x 7 = 49 detectors.

In table 4 the coincidence results of first order type, measured by taking as central detectors some of the detectors placed in the last but one array contour, are shown. As one can see, there is a drastic decrease in the number of coincidences from the center to the periphery of the array detector.

3.3. The transverse momentum corresponding to the narrow neutron group measured by the aid of the new array detector

The transverse momentum distribution corresponding to the neutrons within the narrow neutron group has been determined from the data furnished by detectors disposed along two lines passing through the central #1 detector. One line parallel to x axis contains the detectors #58, #32, #14, #4, #1, #8, #22, #7. The data corresponding to this line are presented in Fig.6, **a, b.** The other line, parallel to y axis, contains the detectors: #66, #38, #18, #6, #1, #2, #10, #26, #50 (see Fig.7, **a, b**).

In Fig 6**a,** and in Fig 7**a,** the fit was done using the Gauss function (1).

$$(1)\quad y = \frac{A}{\sqrt{2\pi\sigma^2}} e^{\frac{-(x-x_c)^2}{2\sigma^2}}$$

$$(2)\quad y = y_0 + \frac{A}{\sqrt{2\pi\sigma^2}} e^{\frac{-(x-x_c)^2}{2\sigma^2}}$$

In Fig. 6**b** and in Fig. 7**b** the fit was done using the Gauss function (2).

In the second form, y_0 is a background found by fit to be near 70 counts. This value is close to the mean value of 64 counts, corresponding to the outer 31 detectors of the array. Expressing $p_\perp$ through σ, from the fit follows that in Fig.6**a**, Fig.7**a** the value of $p_\perp$ is about 2 times larger ($p_\perp \approx 11.5 \pm 1.5$ MeV/c) than in Fig.6**b**, Fig.7**b** ($p_\perp \approx 6 \pm 1.2$ MeV/c). The $p_\perp$ observed in previous experiment [8], is $p_\perp \approx 12 \pm 1$ MeV/c.

From these data follows the importance of the background on which the narrow neutron peak is superposed. This background may correspond to evaporation neutrons, pre-emission of single neutrons within a broader distribution etc. (see ref. [3, 11]).

3.4. Estimation of neutron pair pre-emission percentage P_{nn} within the narrow neutron group

Taking into account the results of previous #3.3 paragraph, P_{nn} was estimated in 2 variants: 1. By assuming a background of 64 counts within the range of #1-#49 central detectors. 2. By assuming that the background is 0.

1. Extracting the background of 64 counts, a number of 2447 counts remain in the #1 to #49 detector zone. Subtracting further a 10% cross talk background (obtained from data of Table 3), it follows a net number of 2203 ± 75 detected neutrons. Considering the number of detected coincidences 314.7 ± 30 (Table 3) and dividing by squared neutron detection efficiency $\varepsilon^2 = 0.34^2$ the number of pre-emitted neutron pairs $N_2 = 2721 \pm 260$ is obtained. The number N_1 of single pre-emitted neutrons can be obtained from: $(N_1 + 2N_2) = (2203 \pm 75)/\varepsilon$. From this relation follows $N_1 = 1038 \pm 340$. The P_{nn} percentage is given by $P_{nn} = N_2/(N_1 + N_2)$, from which $P_{nn} = (72 \pm 10)\%$

2. In the second case, one has to add back the number of 49*64=3136 ± 56 counts which represents the assumed background. Repeating the upper calculations, P_{nn} turns out to be $P_{nn} = (22 \pm 3)\%$.

3.5 Determination of the differential cross-section for n-n pre-emission

The n-n coincidence data allow to obtain, the differential cross-section for n-n pre-emission, by taking into account the solid angles corresponding to each type of n-n coincidence. In Tables 1-3 we considered the 1-9 central detectors, conditioning the first order, 2-nd order and 3-rd order coincidences. Each such a central detector has 8 first order neighbors, 16- second order neighbors and 24 third order neighbors. For reason of solid angle normalization, if the number of first order coincidences remains unchanged, the number of second order coincidences have to be divided by 2, and the number of third order coincidences have to be divided by 3. In Fig. 8, the points with error bars represent the $d^2\sigma_{nn}(\theta_1,\theta_2)/d\Omega_1 d\Omega_2$ cross-sections for the 3 types of coincidences, obtained from Tables 1-3 using data for conditioning detector #1. In the same figure, the points marked 1, 2, 3 and the corresponding slope, represent the neutron transverse momentum distribution plotted in Figs. 6 and 7. These points were obtained by taking the average values of both negative (1', 2', 3') and positive (1", 2", 3") transverse momentum branches presented in both Fig. 6b and Fig. 7b. The reasons for this comparison are the following: 1. The data in Figs. 6, 7 due to the way of the measurements were done, are normalized to solid angle. 2. In both cases, the main quantity one is dealing with, is the transverse momentum. In the first case the transverse momentum is measured by detecting single neutrons. In the second case, the transverse momentum is measured by detecting first order, second order and third order coincidences. The fact that the $d^2\sigma_{nn}(\theta_1,\theta_2)/d\Omega_1 d\Omega_2$ values are close to the red slopes, points out to a phenomenon that governs at the same time the behavior of transverse momentum and the behavior of n-n coincidences.

In Fig 9 are plotted $d^2\sigma_{nn}(\theta_1, \theta_2)/d\Omega_1 d\Omega_2$ coincidences obtained by interchanging det. #1 with det # 2,4,6,8 (Fig 9a), and by interchanging det#1 with det. # 3,5,7,9. The change in slope of coincidence points in comparison with Fig 8 may be an indication for

neutron-neutron correlation. We intend to investigate further this point in order to understand better the degree of n-n correlation.

In contrast to the n-n coincidence data, the cross-talk data processed in the same manner for getting the cross-sections, are totally in disagreement with the red slopes, as one can see in Fig. 10.

4. Summary

- For the first time, a large n-n coincidences effect has been observed for the neutrons pre-emitted in Si (^{11}Li, fusion).

- The measurement with the array detector allowed a new determination with increased resolution of the transverse momentum distribution for the neutrons within the narrow group. The best fit of the experimental data was obtained by allowing a background term in the Gauss function. In this case the transverse momentum $p_\perp$ expressed by σ of the distribution is $p_\perp \approx 6 \pm 1.2$ MeV/c. About 2 times larger value of $p_\perp$, comparable with the value of the previous experiment [8], was obtained by forcing the fit without a background term.
- The n-n coincidence data processed by considering a background on which the narrow neutron group is superposed, allowed to obtain for P_{nn}, the percentage for neutron pair pre-emission, the value $P_{nn}=(72 \pm 10)\%$. Without subtraction of this background P_{nn} turns out to be $P_{nn}=(22 \pm 3)\%$.

- The differential cross-section $d^2\sigma_{nn}(\theta_1,\theta_2)/d\Omega_1 d\Omega_2$ for two neutron pre-emission as a function on the angle θ_2 between the momenta of neutrons has been tentatively determined. Good agreement between this cross-section and the transverse momentum distribution of the neutrons, has been noticed. In contrast to the n-n coincidence data, the cross-talk data processed in the same manner for getting the cross-sections, are totally in disagreement with the slope of the neutron transverse momentum distribution. It was also observed a change in the slope of n-n coincidence data, by interchanging det. #1 with det. #2,4,6,8 and #3,5,7,9. This may be an indication for n-n correlation.

References

[1] I.Tanihata, H.Hamagaki, O.Hashimoto, S.Nagamya, Y.Shida, N.Yoshikawa, K.Sugimoto, T.Kobayashi, D.E.Greiner, N.Takahashi, Y.Nojiri, Phys.Lett.**160B**, 380 (1985)

[2] M.Petrascu, A.Isbasescu, H.Petrascu, I.Tanihata, T.Kobayashi, Balkan Physics Letters **3(4)**, 214 (1995)

[3] M.Petrascu , I.Tanihata , T.Kobayashi , A.Isbasescu , H.Petrascu , A.Korsheninnikov, E.Nikolski , S.Fukuda , S.Kumagai , T.Momota , A.Ozawa , K.Yoshida , C.Bordeanu, I.Lazar , I.Mihai , G.Vaman , M.Giurgiu, Phys.Letters **B405**, 224-229 (1997)

[4] M.Petrascu, *Proc. Int. Summer School,Predeal, Romania, Aug.28-Sept.9(1995)*, A.A.Raduta, D.S.Delion, I.I.Ursu eds. (World Sci. Singapore) (1996)

[5]. M.Petrascu , I.Tanihata , T.Kobayashi, A.Isbasescu , H.Petrascu , A.Korsheninnikov , E.Nikolski , S.Fukuda , S.Kumagai , T.Momota , A.Ozawa , K.Yoshida . C.Bordeanu , I.Lazar , I.Mihai , G.Vaman , M.Giurgiu, Prep.RIKEN-AF-NP-237 (1996)

[6] M.Petrascu,I.Tanihata,T.Kobayashi, A.Isbasescu, H.Petrascu, A.Korsheninikov, E.Nikolski, M.Fujimaki, H.Kumagai,A.Ozawa,T.Suzuki, K.Yoshida,C.Bordeanu, M.Giurgiu, I.Lazar,I.Mihai,G.Vaman, Rom. Journal of Phys. vol **43**, 307 (1998)

[7] M.Petrascu, C.Bordeanu, M.Giurgiu, A.Isbasescu, J. Phys. **G 25**, 799 (1999)

[8] M.Petrascu, I.Tanihata, T.Kobayashi, A.Isbasescu, H.Petrascu, A.Korsheninnikov, E.Nikolski, Zs. Fulop, H.Kumagai, K.Morimoto, A.Ozawa, T.Suzuki, F.Tokanai, K.Yoshida, Haining Wang, C.Bordeanu, M.Giurgiu, I.Lazar, I.Mihai, G.Vaman, Rom. Journal of Phys.- vol 44, no.1-2, Supplement, 83 (1999)

[9] H.Petrascu, H.Kumagai, I.Tanihata, M.Petrascu, Z.S.Fulop, Rom. Journal of Physics –vol.**44**, no. 1-2, Supplement, 105 (1999)

[10] M.Petrascu, I.Tanihata, I.Cruceru, C.Bordeanu, H.Kumagai, A.Isbasescu, D.Mangeac, K.Morimoto, F.Negoita, H.Petrascu, D.Stanescu, R.Ruscu, C.Timis, M.Giurgiu, Rom. Journal of Phys.- vol **44**, no.1-2, Supplement, 115 (1999)

[11] M.Petrascu, *Proc. Int.Summer School, Predeal, Romania, Aug.24 – Sept.5 (1998)*, A.A.Raduta, S.S.Stoica, I.I.Ursu eds. (World Sci. Singapore), 268 (1999)

[12] M.V.Zhukov, V.Danilin, D.V.Fedorov, J.M.Bang, I.J.Thomson, J.S.Vaagen Phys.Rep. **231**, 151 (1993)

[13] M.I.Podgoretsky, Particle&Nuclei **20**, 628 (1989)

[14] R. Ghetti et al. Phys.Rev. **C62,** 037603 (2000)

[15] see A. Gavron, Phys. Rev. **C20** 230 (1980)

Table 1: Determination of first order n-n coincidences in ^{11}Li + Si. Beam energy range: 12.2-14.2 AMeV (at the target entrance). Neutron energy range 6-16 MeV. Analysis file:spenc1g.ana. Runs: 005,006,007,009,010,011,012,013,015,016,017. Cross-talk coeff.: 0.020±0.003

Cond. Det.	Surround Det	Number of coincid.	Monitor CD+SD	Cross-talk Backgr.	n-n coin. Effect	Obs.
#1	2_9	55	215+1336 =1551	31±5.4	24±9.2	
#2	3,4,8,9,10 11,25	38	164+1062 =1226	24.5±4.4	13.5±7.6	E: 1
#3	10_14,4,	33	129+839 =968	19.3±3.5	13.7±6.7	E: 1,2
#4	5,6, 13_15	23	100+757 =857	17.1±3.2	5.9±5.8	E: 1,2,3
#5	14_18,6	34	130+825 =955	19.1±3.5	14.9±6.8	E: 1,4
#6	7,8,17_19	26	94+707= 801	16±3	10±5.9	E: 1,4,5
#7	8,18_22	25	124+714 =838	16,7±3.1	8.3±5.9	E: 1,6
#8	9,21_23	22	86+495= 581	11.6±2.2	10.4±5.2	E: 1,2,6,7
#9	10,22_25	22	96+589= 685	13.7±2.5	8.3±5.3	E: 1,2,8
Total		278		169±11	109±23	

By E it is denoted the exclusion of coincidences with the specified detectors, because they were already taken into account.

In the upper analysis, the coincidences between the central #1 to #9 detectors and the 1-st order neighbors (see the array diagram, Fig.5) were considered. For example the 1-st order neighbors of detector #1, are detectors #2 to #9

Table 2: Determination of second order n-n coincidences in ^{11}Li + Si.. Beam energy range: 12.2-14.2 AMeV, (at target entrance). Neutron energy range 6-16 MeV. Analysis file:spenc1g.ana. Runs: 005,006,007,009,010,011,012,013,015,016,017. Cross-talk coeff.:0.0052±0.001

Cond. Det.	Surround Det	Number of coincid.	Monitor CD+SD	Cross-talk Backgr.	n-n coin. Effect	Obs.
#1	10_25	30	215+1983 =2198	11.4±2.4	18.6±6	
#2	26_28,12_ 15,5_7,21 _24,48,49	27	164+1976 =2140	11.1±2.3	15.9±5.7	
#3	26_33,5_9 25,49	21	129+1897 =2026	10.5±2.2	10.5±5	
#4	10_12,30_ 34,16_19 7_9,25	26	100+2208 =2308	12.0±2.5	14±5.7	
#5	13,31_39, 7_9,19	22	130+1559 =1689	8.8±1.9	13.2±5	E: 2,3
#6	13_16,36_ 40,20_23, 9	20	94+1586= 1680	8.8±1.9	11.2±4.8	E: 2,3
#7	9,17,23,37 _45	11	124+1189 =1313	6.8±1.5	4.2±3.6	E: 2_5
#8	24,25,10,11 ,17_20,42_ 46	24	86+1375 =1461	7.6±1.7	16.4±5.2	E: 3_5
#9	11,21,26, 27,43_49	9	96+1053 =1149	6.0±1.3	3±3.2	E: 3_7
Total		190		83±6	107±15	

In the upper analysis, the coincidences between the central #1 to #9 detectors and the 2-rd order neighbors (see the array diagram, Fig.5) were considered. For example the 2-nd order neighbors of detector #1, are detectors #10 to #25

Table 3: Determination of 3-rd order n-n coincidences in ^{11}Li + Si. Beam energy range: 12.2-14.2 AMeV (at target entrance) Neutron energy range 6-16 MeV. Analysis file:spenc1g.ana. Runs: 005,006,007,009,010,011,012,013,015,016,017. Cross-talk coeff.: 0.0017±0.0007

Cond. Det.	Surround Det	Number of coincid.	Monitor CD+SD	Cross-talk Backgr.	n-n coin. Effect	Obs.
#1	26_49	19	215+2024 =2239	3.8±1.7	15.2±4.7	
#2	16_20,29_ 34,42_47, 50_53,79, 80	17	164+1924 =2088	3.5±1.6	13.5±4.4	
#3	16_24,50_ 60,34,48, 80	10	129+1952 =2081	3.5±1.5	6.5±3.5	
#4	20_24,26_ 29,35_40, 48,49,55_ 61	15	100+2009 =2109	3.6±1.6	11.4±4.1	
#5	10_12,20_ 25,56_68, 30,40	13	130+2044 =2174	3.7±1.6	9.3±3.9	
#6	10_12,30_ 35,41_46, 63_69,24, 25	10	94+2090= 2184	3.7±1.6	6.3±3.5	
#7	10_16, 64_76,24, 25,36,46	14	124+2184 =2308	3.9±1.7	10.1±4.1	
#8	12_16,26_2 8,36_41,71 _77,47_49	19	86+2204 =2290	3.9±1.7	15.1±4.6	
#9	12_20,72_ 80,50_52, 28,42	15	96+2107 =2203	3.7±1.7	11.3±4.2	
Total		132		33.3±4.9	98.7±12.4	
Tot(fo+so +3-o)		600		285.3±14	314.7±30	

In the upper analysis, the coincidences between the central #1 to #9 detectors and the 3-rd order neighbors (see the array diagram, Fig.5) were considered. For example the 3-rd order neighbors of detector #1, are detectors #26 to #49

Table 4: Results on first order n-n coincidences in ^{11}Li + Si, in the array peripheral region.Beam energy range: 12.2-14.2 AMeV (at the target entrance). Neutron energy range 6-16 MeV. Analysis file:spenc1ja.ana. Runs: 005,006,007,009,010,011,012,013,015,016,017. Cross-talk coeff.: 0.020±0.003

Cond. Det.	Surround Det	Number of coincid.	Monitor CD+SD	Cross-talk Backgr.	n-n coin. Effect	Obs.
#26	10_11,25,27, 49,50,51	20	94+805 =899	18±2.8	2±5	
#29	12,28,30,52_ 56	13	56+597 =653	13±2.1	0±4.1	
#32	13_15,31, 33 57_59	14	81+827= 908	18.1±2.9	-4.1±4.7	
#35	16,34,36,60_ 64	19	75+550= 625	12.5±2	6.5±4.8	
#38	17_19,37, 39, 65_67	26	97+841= 938	18.8±3	7.2±5.9	
#41	20,40,42, 68_ 72	15	54+484= 538	10.8±1.7	4.2±4.2	
#44	21_23, 43, 45 73_75	17	73+764= 837	16.7±2.6	0.3±4.9	
#47	24, 46,48,76_ 80	19	62+539= 601	12.±1.9	7±4.8	
Total		143		119.9±6.8	23.1±14	

In the upper analysis, the coincidences between #26, #29 ..to #47 detectors , placed on the last but one array contour, and their 1-st order neighbors (see the array diagram) were considered. For example the 1-st order neighbors of detector #29, are detectors #52_56, #30, #12, and #28.

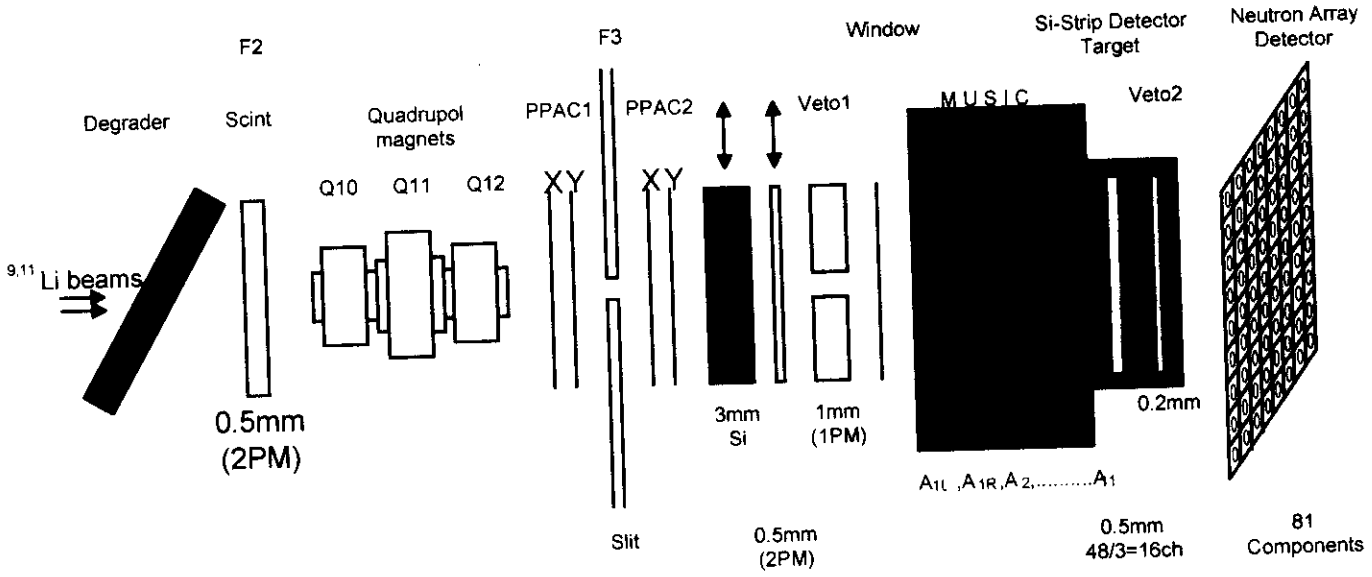

Fig. 1: The general set-up of the experiment. In this arrangement, a thin scintillator mounted at the F2 focus of RIPS, two position-sensitive Parallel Plate Avalanche Counters PPAC1, PPAC2, two removable detectors (Si det., 0.5 mm scintillator) a Veto1 scintillator, having a 2x2 cm^2 hole, a MUSIC chamber with a Si-strip (SiS) detector-target and a Veto2 Si detector mounted inside, and a 81 components neutron array detector were used. As trigger, the coincidences $F2 * PPAC2 * \overline{Veto1} * SiS * \overline{Veto2}$ were chosen.

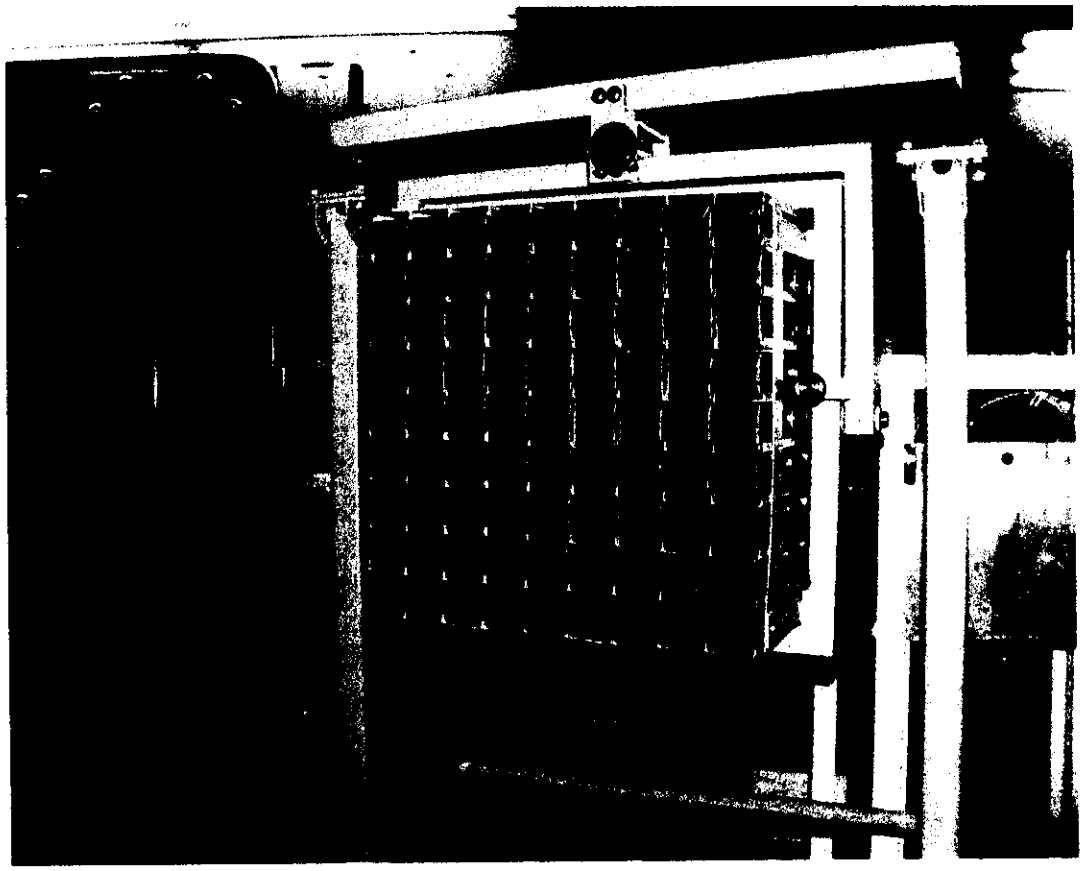

Picture 1. A view of the neutron array detector, built within the cooperation agreement between the Institute of Physics and Nuclear Engineering, Romania and RIKEN, Japan.
It consists of 81 detectors, made of 4 x 4 x12 cm^3 BC-400 crystals , mounted on XP2972 phototubes.

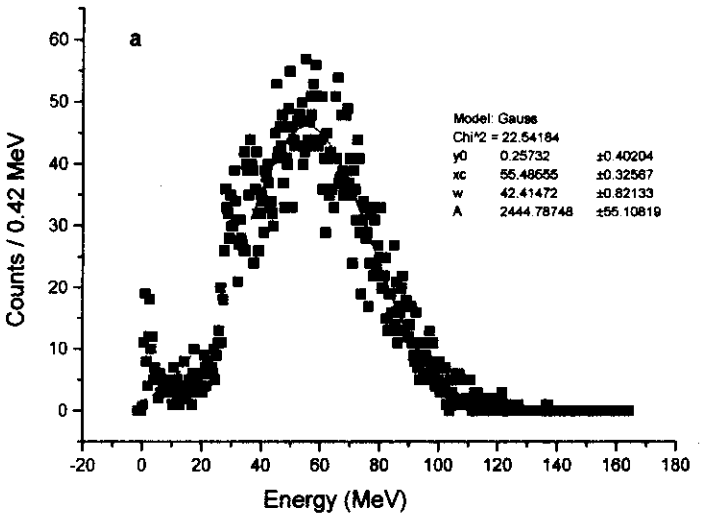

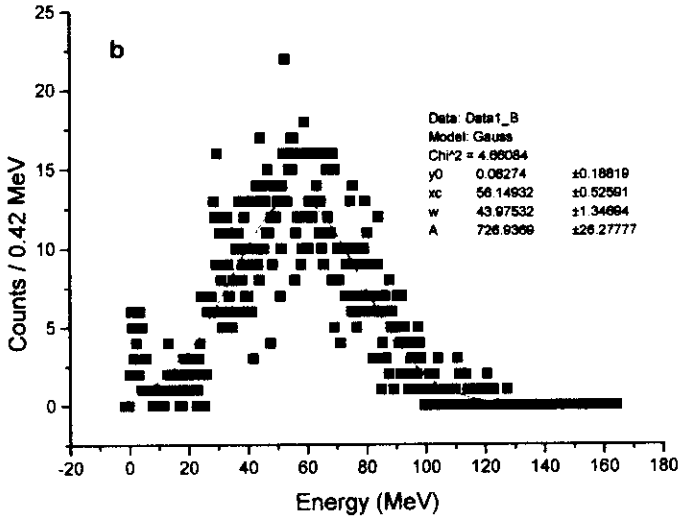

Fig. 2. The pulse height spectrum of target for ^{11}Li + Si in the 12.2-14.2 MeV beam energy range, gated by:
a: 6-16 MeV neutron energy range.
b: 0.7-6 MeV neutron energy range.

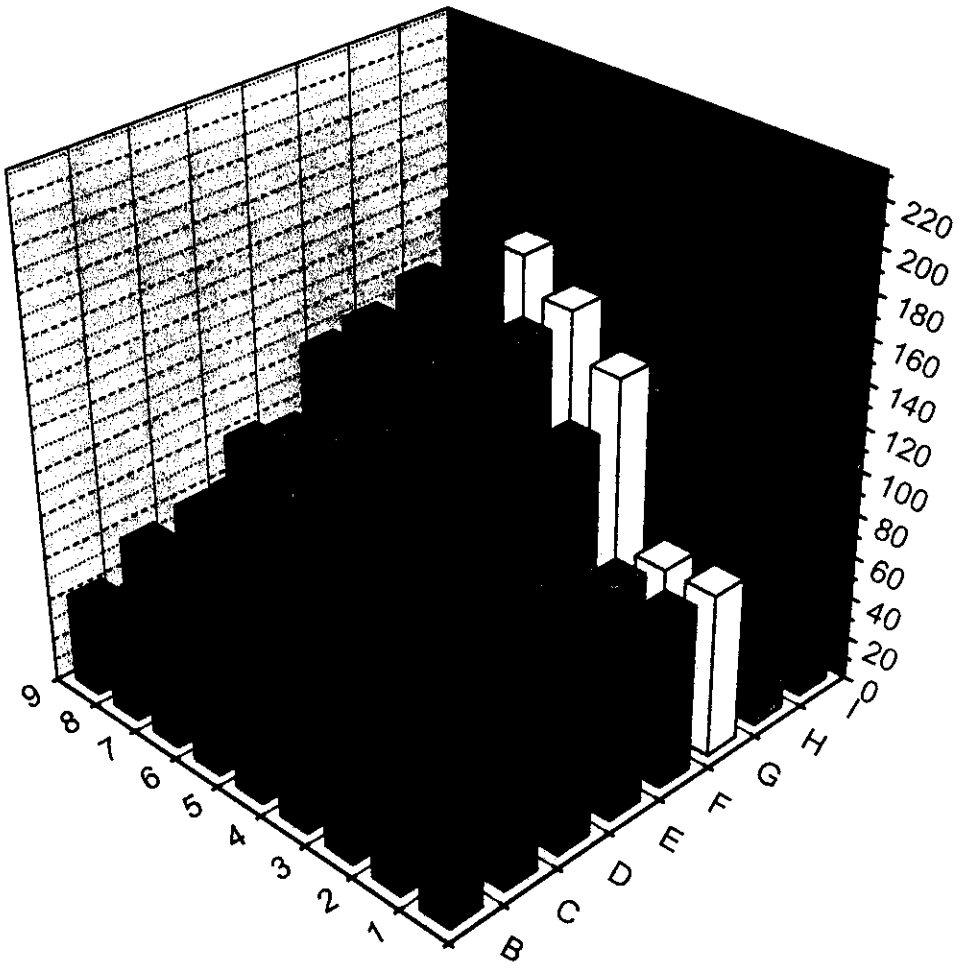

Fig. 3. The position distribution of neutrons from Si(^{11}Li, fusion), measured by the aid of the array detector. ^{11}Li beam energy range: 12.2 –14.2 AMeV. Neutron energy range: 6-16 AMeV.

As one can see, there is a very pronounced distribution in forward direction. The highest peak corresponds to the central #1 detector of the array (215 counts). The mean number on the outer contour is 64 counts.

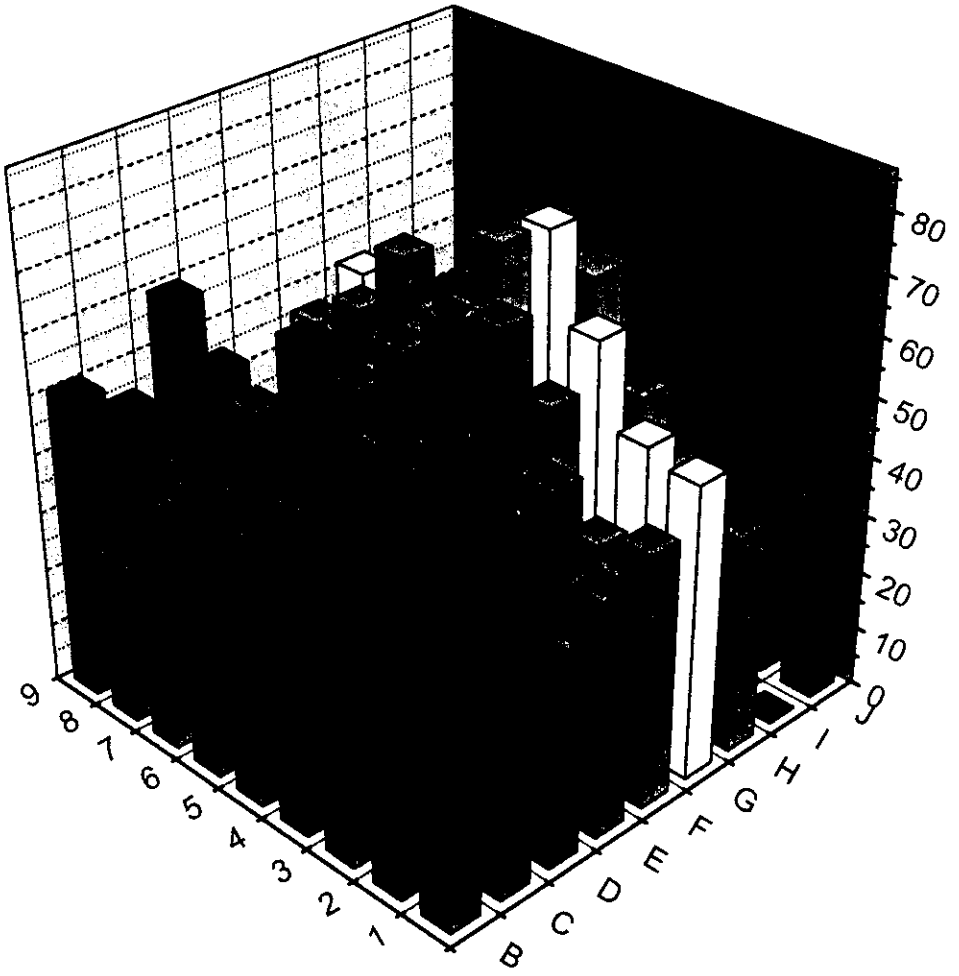

Fig.4. The position distribution of neutrons from Si(^{9}Li, fusion), measured by the aid of the array detector, in conditions similar to those of Fig.2. This distribution is almost uniform, without any pronounced tendency in the forward direction. These data were used for the cross-talk coefficients determination.

54	53	52	51	50	81	80	79	78
55	29	28	27	26	49	48	47	77
56	30	12	11	10	25	24	46	76
57	31	13	3	2	9	23	45	75
58	32	14	4	1	8	22	44	74
59	33	15	5	6	7	21	43	73
60	34	16	17	18	19	20	42	72
61	35	36	37	38	39	40	41	71
62	63	64	65	66	67	68	69	70

Fig.5. The numbering scheme of the neutron array detector. The detector labeled #1 was placed in the center. Detectors #2-#9 are the closest detectors surrounding detector #1. Then follows the second circle, formed by detectors #10 - #25, the 3-rd circle formed by detectors #26 - # 49, and the 4-th circle formed by detectors #50 - #81.

Coincidences between some detector and the closest surrounding detectors, are considered in this paper as "first order coincidences". Coincidences between some detector and the detectors forming the second circle are considered second order coincidences, and so on.

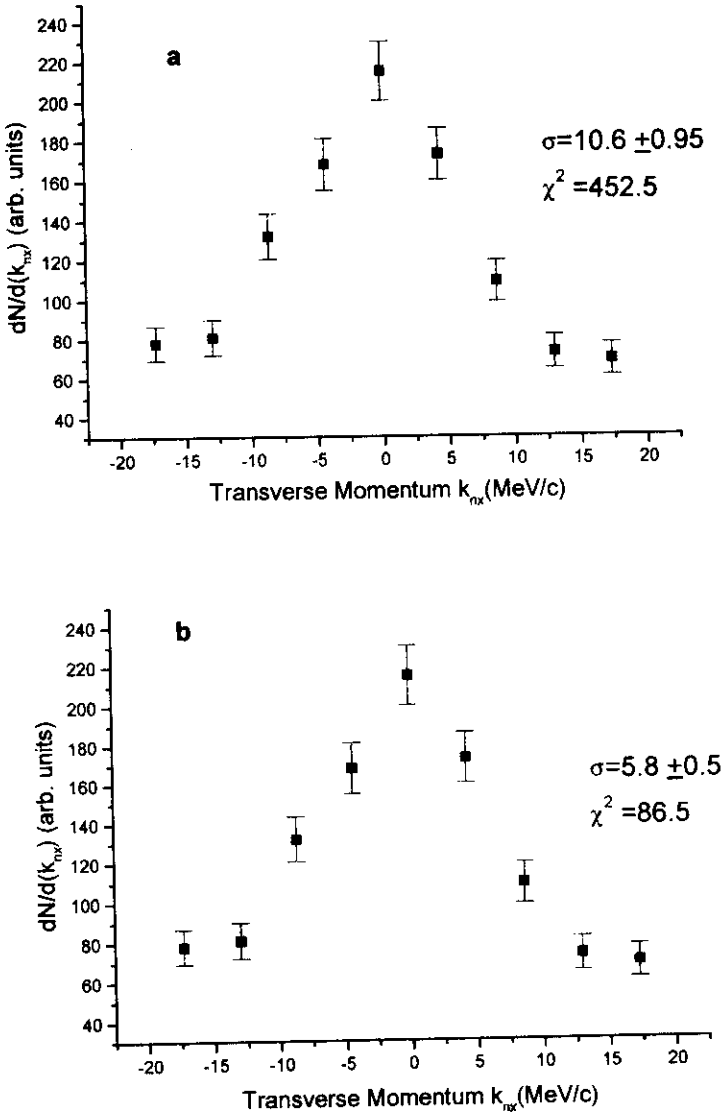

Fig.6. **a, b:** transverse momentum distribution of the pre-emitted neutrons in Si(^{11}Li, fusion), (within the forward peak), measured along the line parallel to x axis of the array, containing the detectors #58, #32, #14, #4, #1, #8, #22, #44, #74, (see Fig. 5).

In **a, b** the Gaussian fit using respectively $y = \frac{A}{\sqrt{2\pi\sigma^2}} e^{\frac{-(x-x_c)^2}{2\sigma^2}}$ and $y = y_0 + \frac{A}{\sqrt{2\pi\sigma^2}} e^{\frac{-(x-x_c)^2}{2\sigma^2}}$ was done. Expressing $p_\perp$ through σ, from the fit follows that in **a** the value of $p_\perp$ is about 2 times larger than in **b,** but the fit in **b** appears to be more reliable since the χ^2 value is essentially lower.

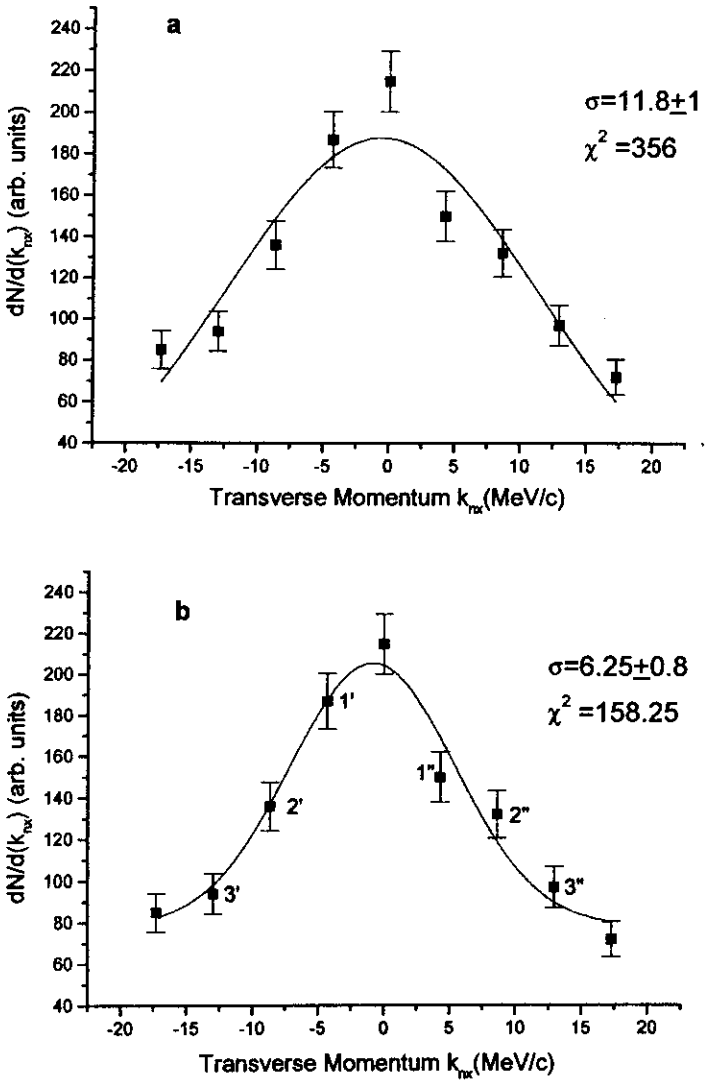

Fig.7. **a, b:** transverse momentum distribution of the pre-emitted neutrons in Si(^{11}Li, fusion), (within the forward peak), measured along the line parallel to y axis of the array, containing the detectors #50, #26, #10, #2, #1, #6, #18, #38, #66, (see Fig. 5).

In **a, b** the Gaussian fit using respectively $y = \frac{A}{\sqrt{2\pi\sigma^2}} e^{\frac{-(x-x_c)^2}{2\sigma^2}}$ and $y = y_0 + \frac{A}{\sqrt{2\pi\sigma^2}} e^{\frac{-(x-x_c)^2}{2\sigma^2}}$ was done. Expressing $p_\perp$ through σ, from the fit follows that in **a** the value of $p_\perp$ is about 2 times larger than in **b**, but the fit in **b** appears to be more reliable since the χ^2 value is essentially lower.

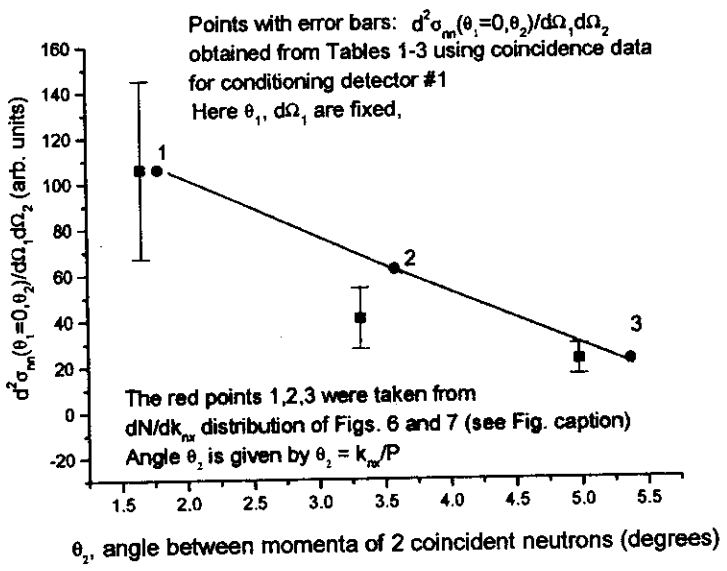

Fig.8. The points with error bars are $d^2\sigma_{nn}/d\Omega_1 d\Omega_2$ cross-sections obtained from first, second and third order coincidences of Tables 1-3, considering the conditioning detectors #1.
The points marked 1, 2, 3 were obtained by taking the average values of both negative (1', 2', 3') and positive (1", 2", 3") branches of the distributions presented in both Fig. 6b and Fig. 7b. Afterwards, the average background corresponding to the last contour of the array, equal to 64 counts was subtracted. The distributions in Fig. 6 and 7, due to the way in which measurements were performed, are solid angle normalized... The $d^2\sigma_{nn}/d\Omega_1 d\Omega_2$ cross-section values were normalized to the value of point #1. One can see that the cross-section values for 2-nd and third order coincidences are close to the slope corresponding to the transverse momentum distribution.

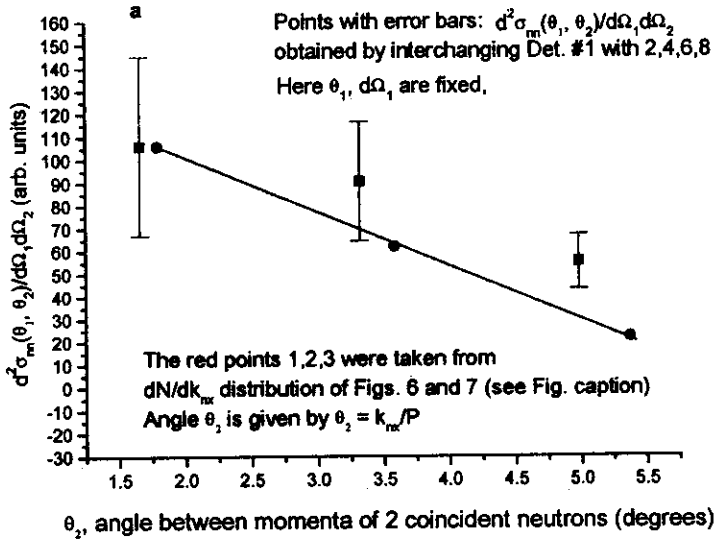

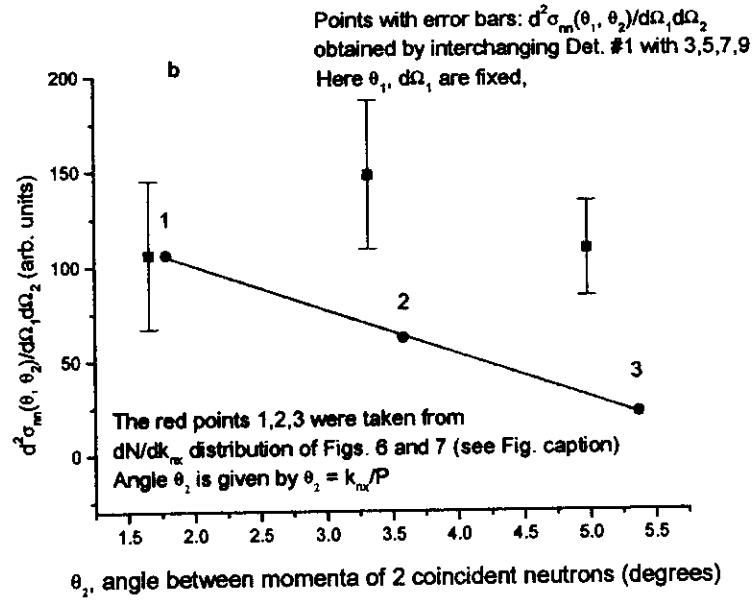

Fig.9. The points with error bars are $d^2\sigma_{nn}/d\Omega_1 d\Omega_2$ cross-sections obtained from first, second and third order coincidences by interchanging in a: Det #1 with 2,4,6,8, and in b: Det. #1 with 3,5,7,9
The points marked 1, 2, 3 were obtained by taking the average values of both negative (1', 2', 3') and positive (1", 2", 3") branches of the distributions presented in both Fig. 6b and Fig. 7b. Afterwards, the average background corresponding to the last contour of the array, equal to 64 counts was subtracted. The distributions in Fig. 6 and 7, due to the way in which measurements were performed, are solid angle normalized... The $d^2\sigma_{nn}/d\Omega_1 d\Omega_2$ cross-section values were normalized to the value of point #1.
The change in the $d^2\sigma_{nn}/d\Omega_1 d\Omega_2$ slope with respect to the 1, 2, 3, line in comparison with Fig. 8, may be an indication for neutron-neutron correlation.

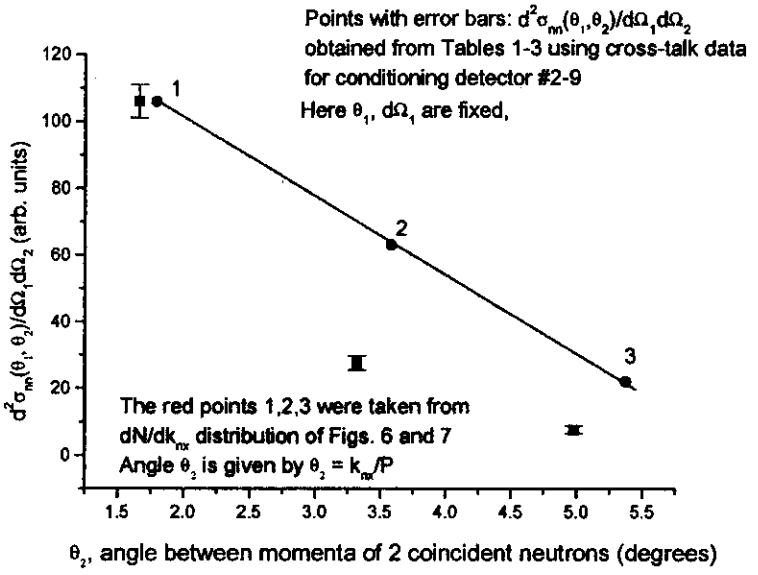

Fig.10 The points with error bars are $d^2\sigma_{nn}/d\Omega_1 d\Omega_2$ cross-sections obtained from first, second and third order cross-talks of Tables 1-3, considering the conditioning detectors #2-#9.
The points marked 1, 2, 3 was obtained by taking the average values of both negative (1', 2', 3') and positive (1", 2", 3") branches of the distributions presented in both Fig. 6b and Fig. 7b. Afterwards, the average background corresponding to the last contour of the array, equal to 64 counts was subtracted. The distributions in Fig. 6 and 7, due to the way in which measurements were performed, are solid angle normalized... The $d^2\sigma_{nn}/d\Omega_1 d\Omega_2$ cross-section values were normalized to the value of point #1. One can see that the cross-section values for 2-nd and third order cross-talks are far apart to the slope corresponding to the transverse momentum distribution.